Geo-Mar Lett (2012) 32:489–499
DOI 10.1007/s00367-012-0283-1

ORIGINAL

Sidescan sonar imagery of widespread fossil and active cold seeps along the central Chilean continental margin

Ingo Klaucke · Wilhelm Weinrebe · Peter Linke · Dirk Kläschen · Jörg Bialas

Received: 19 May 2011 / Accepted: 20 February 2012 / Published online: 7 March 2012

Abstract The central Chilean subduction zone between 35°S and 37°S was investigated in order to identify, document and possibly understand fluid flow and fluid venting within the forearc region. Several areas were mapped using multibeam bathymetry and backscatter, high-resolution sidescan sonar, chirp subbottom profiling and reflection seismic data. On a subsequent cruise ground-truthing observations were made using a video sled. In general, this dataset shows surprisingly little evidence of fluid venting along the mid-slope region, in contrast to other subduction zones such as Central America and New Zealand. There were abundant indications of active and predominantly fossil fluid venting along the upper slope between 36.5°S and 36.8°S at the seaward margin of an intraslope basin. Here, backscatter anomalies suggest widespread authigenic carbonate deposits, likely the result of methane-rich fluid expulsion. There is unpublished evidence that these fluids are of biogenic origin and generated within the slope sediments, similar to other accretionary margins but in contrast to the erosional margin off Central America, where fluids have geochemical signals indicating an origin from the subducting plate.

Introduction

Fluids play an important role in a number of processes at active continental margins. Fluids contribute to the lubrication of faults and plate boundaries and consequently influence the occurrence, distribution and magnitude of earthquakes (Hubbert and Rubey 1959; Miller 2002; Ranero et al. 2008). They can weaken sediment cohesion and help trigger submarine landslides (e.g. Dugan and Flemings 2000; Sultan et al. 2004). Fluid flow often results in the accumulation of hydrocarbons in sediments at continental margins, and their emanation at the seafloor constitutes the basis for complex ecosystems (e.g. Paull et al. 1984). Despite these implications, our understanding of the role of fluids in these processes is still rather rudimentary. Difficulties arise in combining large-scale, indirect observations of fluids by seismic or electromagnetic methods with detailed geochemical characterisation of the fluids. In the absence of coring or drilling, fluid sampling can only be carried out at sites where fluids seep out at the seafloor. Locating such sites is ideally carried out with sidescan sonar mapping (e.g. Sahling et al. 2008; Klaucke et al. 2010), which can even provide indications for current seep activity (e.g. Klaucke et al. 2005).

Ranero et al. (2008) have recently integrated various datasets of studies on the Pacific margin of Central America and proposed a hydrological model for erosional active margins. They suggest that fluids from subducting sediments mainly migrate along normal faults and emanate at the mid-slope of the forearc region, forming many cold seeps (cf. Sahling et al. 2008). Although some clustering was observed, the cold seeps were relatively evenly distributed in a band several tens of kilometres wide and stretching for hundreds of kilometres along the Central American margin. This observation differs from the expected seep distribution of other accretionary margin fluid circulation models where fluids would mainly flow along the décollement and emanate at the toe of the accretionary prism (Moore and Vrolijk 1992; Carson and Screaton 1998). Such scenarios have been documented for the Barbados

Responsible guest editors: M. De Batist and O. Khlystov

I. Klaucke (✉) · W. Weinrebe · P. Linke · D. Kläschen · J. Bialas
GEOMAR | Helmholtz Centre for Ocean Research Kiel,
Wischhofstrasse 1-3,
24148 Kiel, Germany
e-mail: iklaucke@geomar.de

accretionary prism (Henry et al. 1990) and the Nankai Trough (Henry et al. 2002), with the latter showing evidence for fluid expulsion in a variety of tectonic settings across and along the margin (Kobayashi 2002). More recent studies of cold seeps at accretionary margins, however, revealed evidence that widespread fluid expulsion exists mainly at the summits of accretionary ridges (e.g. Johnson et al. 2003; Crutchley et al. 2010; Klaucke et al. 2010) and not necessarily at the toe of the accretionary prism. Unfortunately, to date there are no comprehensive, high-resolution inventories of cold seeps along accretionary active margins.

This study presents mainly geophysical (multibeam bathymetry, sidescan sonar, chirp subbottom profiler) data with ground-truth observations of newly discovered active and fossil cold seeps on the central Chilean continental margin between 35°S and 37°S. The occurrence of these seeps on the upper continental slope might further challenge the current models of fluid circulation at accretionary margins. However, geochemical data on the origin and nature of these fluids are not yet available.

Geological setting and previous work

The study area offshore Chile is part of the Andes subduction zone, where the Nazca Plate is being subducted beneath the South American Plate at a rate of 80 mm/year (Fig. 1; DeMets et al. 1994). This part of the Andes subduction zone underwent subduction erosion until at least the Middle Miocene (Kukowski and Oncken 2006) or even until the Pliocene (Melnick and Echtler 2006). Continuing climate cooling since the Miocene and uplift of the Andean Cordillera led to increased sediment input into the trench (Melnick and Echtler 2006) and ultimately to the establishment of an accretionary wedge within the last 1–2 million years (Bangs and Cande 1997). Consequences of this evolution of the margin are still visible in the present-day bathymetry. The Andean slope shows two distinct elements (Fig. 1). The eastern part of the slope between the shelf break and roughly 2,000 m water depth is characterised by a relatively smooth topography that is dissected by NE-SW-trending faults and deeply cut sinuous canyons, while the western part below 2,000 m water depth and down to the trench is characterised by a rough topography with subparallel, N-S-trending ridges (Fig. 1). The eastern part of the margin consists of continental basement rocks that are overlain in the forearc region by sedimentary rocks of maximum age decreasing from north to south. North of 38°N, and within the study area, the oldest sediments are Miocene in age. The South American continental margin south of Valparaiso is dissected by a number of slope canyons leading to the development of submarine fans at the foot of the slope (Thornburg et al. 1990). Turbidity currents have spread across the trench where up to 2.5-km-thick successions of trench-fill sediments have been observed (Bangs and Cande 1997). In the western part of the slope, seawards of the continental crust, is a 20–30 km wide accretionary wedge that probably formed within the last 1–2 Ma. Geersen et al. (2011) analyzed the current tectonic regime of the south Chilean forearc and determined strong kinematic coupling for the north Concepcion segment evidenced by out-of-sequence thrust faulting and large earthquakes, while the south Concepcion segment shows currently inactive normal faults. Normal faults are considered to provide easier fluid pathways than do thrust faults (Behrmann 1992). Although cold seeps have been documented in almost all subduction zones worldwide, data on cold seeps offshore Chile are extremely sparse except for publications by Sellanes et al. (2008, 2010) that include faunal assemblages typical of cold seeps from an area offshore Concepcion and only part of the present study area. The seeps described in those papers are only at the very edge of a much larger seep province.

Materials and methods

The present study is based on data gathered during cruise JC23 of RV *James Cook* in March/April 2008. These include Simrad EM120 multibeam bathymetry data that complemented a wealth of existing bathymetric data from various other cruises with RV *Sonne*, RV *Meteor* and RV *Vidal Gormaz*. The bathymetric and backscatter amplitude data have been gridded with a 200×200 m cell size.

In addition, high-resolution backscatter information has been obtained using a deep-towed sidescan sonar system. The DTS-1 system operated by GEOMAR is a modified EdgeTech dual-frequency sidescan sonar with integrated subbottom profiler. During cruise JC23B the DTS-1 was run using a 75 kHz centre frequency with a range of 750 m. Survey speeds of 2.5–3.0 knots enabled data processing at 1 m pixel size, thus slightly overestimating the along-track resolution. The subbottom profiler operated with a signal of 2–10 kHz frequency and 20 ms pulse length, providing subbottom penetration of up to 40 m. USBL navigation for the towfish was not available and towfish navigation was consequently calculated using a layback method that takes survey speed into account. The sidescan sonar data have been processed using the Caraibes software package from IFREMER or the PRISM package developed at the National Oceanographic Centre, Southampton (Le Bas et al. 1995).

Ground-truthing of the geoacoustic data was carried out recently during cruise SO210 of RV *Sonne* in September/October 2010 using OFOS (Ocean Floor Observation System); a video sled was towed roughly 1.5 m above the seafloor at a speed of 0.5–0.8 knots. For navigation, the ultra-short baseline

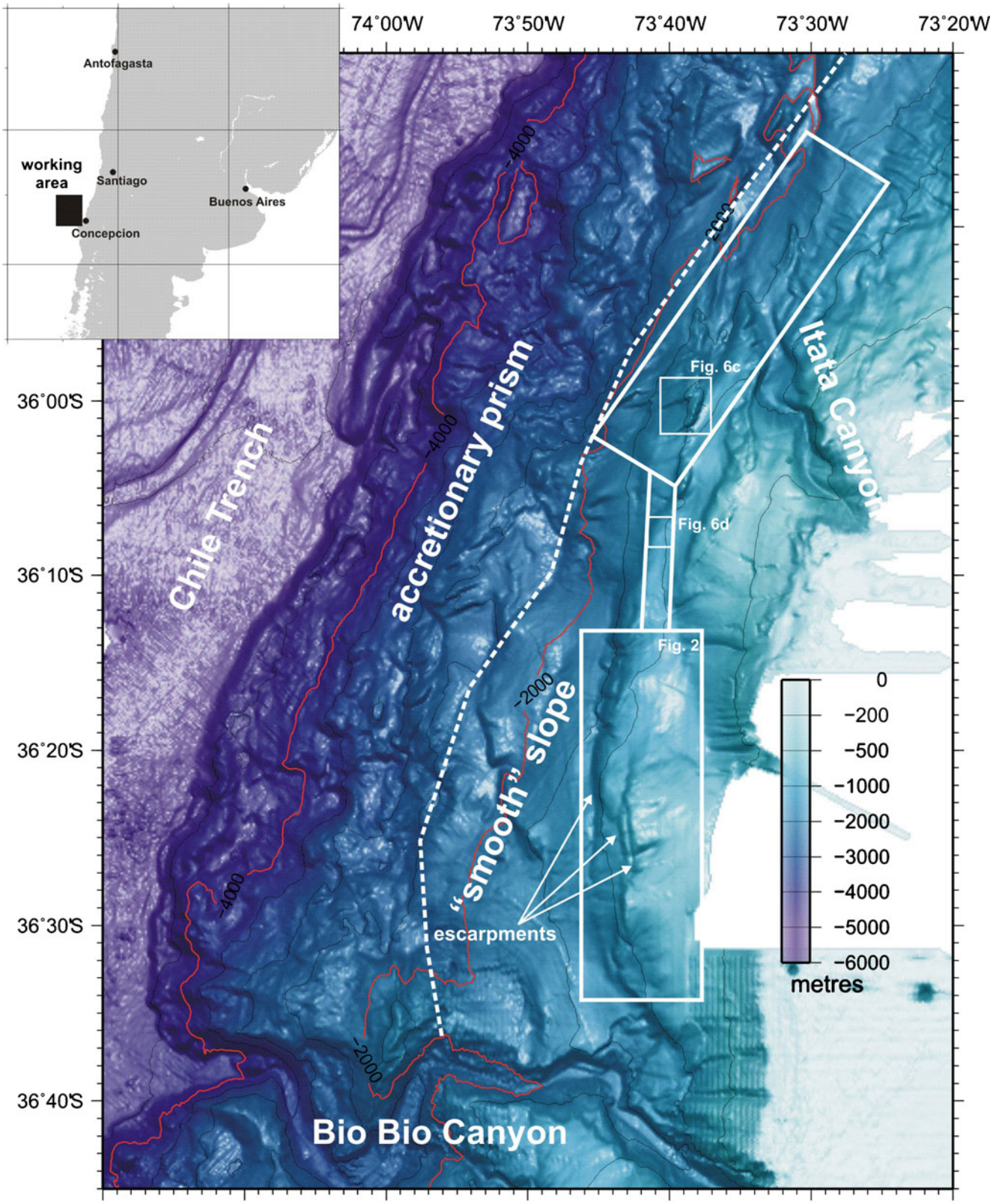

Fig. 1 Shaded bathymetry map of the study area on the Andean continental margin offshore central Chile between 35.5°S and 37°S. Illumination is from the north

USBL-based IXSEA Posidonia system was used in combination with a graphic display program. Limited seismic data of deeper subsurface have been obtained using a 105 cubic inch GI-gun and a four-channel mini-streamer.

Results

Cold seeps at the Andean continental margin between Valparaiso and Concepcion occur in at least two distinct areas based on backscatter intensity maps: along the continental slope north of Bio Bio Canyon and on a large ridge in the vicinity of Itata Canyon (Fig. 1).

North of Bio Bio Canyon

The upper continental slope north of Bio Bio Canyon dips gently towards the west but has three major breaks in slope forming steeper sections. The westernmost break in slope roughly coincides with the 1,250 m depth contour line until about 36°23′S, where it becomes progressively shallower until it disappears at about 36°28′S (Fig. 1). This break in slope is generally very smooth except for two locations at 36°15′S and 36°18′S where it shows evidence for faulting and slumping, and between 36°25′S and 36°28′S where it is dissected by canyons. A second break in slope is situated 2 km further to the east (i.e. further landwards) between 36°21′S and 36°37′S (Fig. 1). It probably continues further south to Bio Bio Canyon but detailed bathymetric data are not available for this area. This second break in slope is situated in variable water depths increasing from north to south. Between 36°23′S and 36°27′S it is doubled by a third break in slope roughly 1 km further inland. These easternmost breaks in slope are dissected by several canyons that follow a WSW–ENE direction that forms an angle both to the slope and to the seafloor lineations further west.

Evidence for cold seeps is mainly found east of the shallowest break in slope between 36°22′S and 36°29′S in water depths ranging between 750 and 850 m. Here, ellipsoidal to elongate patches of high backscatter intensity suggest the presence of either authigenic carbonate precipitates and/or gas-charged sediments (Fig. 2). Two types of seabed features thought to be cold seeps can be distinguished based on the extension of the high backscatter intensity and surface morphology. The first type consists of circular to ellipsoidal patches of increased backscatter intensity that show less than 10 m of relief (Figs. 3 and 4a). The backscatter intensity within each of these patches is not uniform but shows internal variations between medium and high backscatter intensity (Fig. 3). The latter probably correlates with small rounded domes on sediment echosounder profiles (Fig. 4a). Putative cold seeps of this type occur as one cluster centred at 36°28.5′S and 73°40.5′W, and individual patches surrounding the second type of cold seeps. These seeps are currently active as evidenced by backscatter anomalies within the water column of unprocessed sidescan sonar data (Fig. 3, insert a), and anomalous comet-tail reflections on sidescan images (Fig. 3). Video observations of these seeps show the presence of dispersed authigenic carbonates within a mainly fine-grained matrix (Fig. 5a). The presence of sulphidic sediment and bacterial mats indicates recent methane flux, but gas bubbles have not been observed during the video survey in 2010.

The second type of putative cold seeps is characterised by areas of high backscatter intensity of several hundreds of metres in diameter with highly irregular outlines and forming elongate ridges or domes (Fig. 6a, b). The centre of these areas is highly irregular, as shown by many hyperbolic reflections on subbottom profiler records, and may have central pinnacles that are up to 20 m high (Fig. 4b) and 100×250 m wide. Gas flares on raw sidescan sonar data indicate that these cold seeps are also currently active. However, no active gas venting was seen with video observations conducted several years later. These video data show extensive carbonate pavements that are in places covered by a thin veneer of sediment or show cracks underlined by bacterial mats (Fig. 5b) indicating fluid venting activity. Large carbonate boulders have also been observed (Fig. 5c).

The cold seeps described by Sellanes et al. (2008) are at the north-western edge of this major seep province (Fig. 2). They appear as ellipsoidal areas of high backscatter intensity that are not associated with high seafloor relief and are consequently of type 1. The seeps situated just several hundreds of metres further south and documented here for the first time are much larger in surface extent, with indications of authigenic carbonate precipitates and probably fluid flux.

In the vicinity of Itata Canyon

About 50 km further north of the Bio Bio Canyon area, at 36°S, additional cold seeps are found in similar tectonic settings (Fig. 1). In this area the northward extension of the slope break described above abuts against the sinuous Itata Canyon. Itata Canyon was probably linked to the Itata River in the geological past, but a relatively smooth canyon floor suggests it to be inactive now. The path of Itata Canyon is controlled by NNE-SSW-trending faults that are responsible for the formation of two ridges on the continental slope and an intraslope basin (Fig. 1). These ridges are in turn dissected by WSW-ENE-trending faults.

At one location these faults appear to have been the pathway for fluids, occurring as patchy high backscatter intensity around the fault (Fig. 6d) and currently the location of sediment-covered blocks of authigenic carbonate. This fossil cold seep has been imaged for at least 1 km surrounding the surface expression of the fault. The fossil cold seep widens from east to west, reaching a width of about 500 m at the western end of the sidescan sonar profile in Fig. 6d. The maximum westward extension of this fossil cold seep is not known. In addition, isolated, small patches of high backscatter intensity occur some 1,000–1,500 m further to the

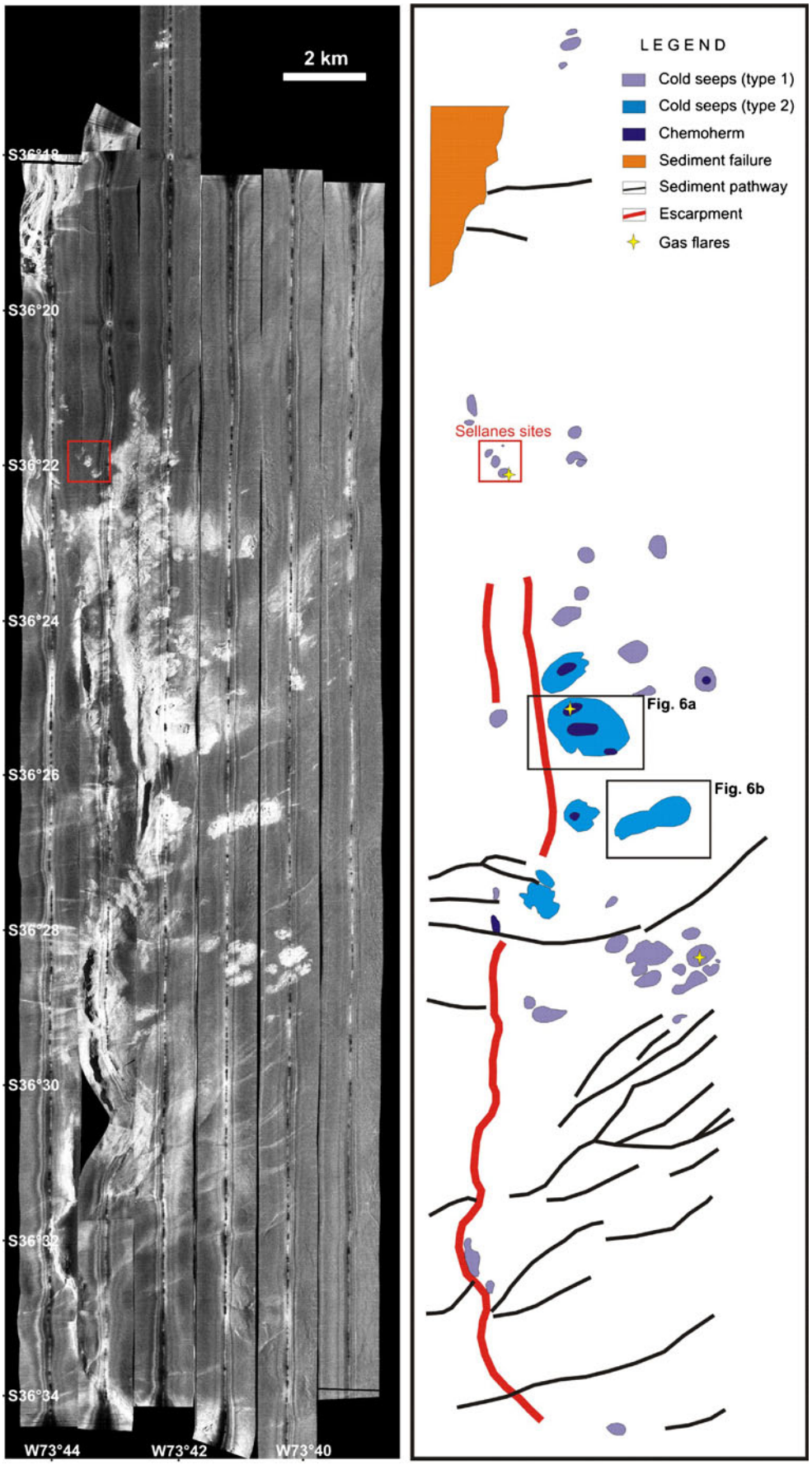

Fig. 2 Sidescan sonar mosaic and geological interpretation of the Talcahuano seep province north of Bio Bio Canyon. High backscatter intensity is white. *Red box* Seeps reported on by Sellanes et al. (2008)

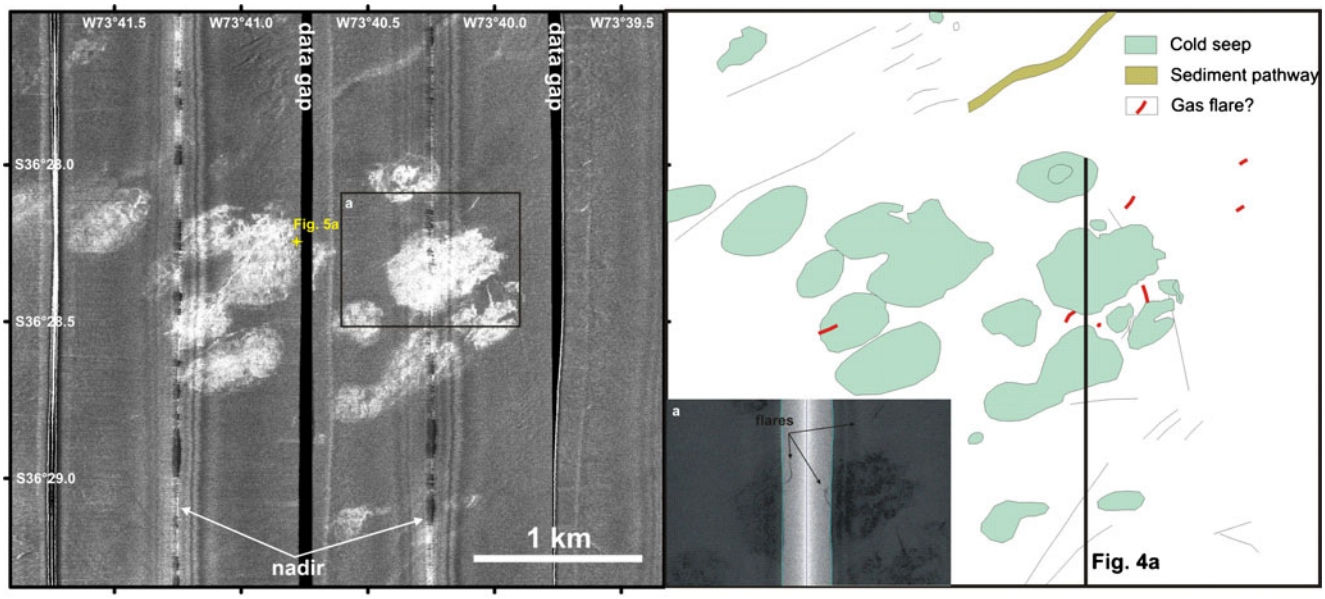

Fig. 3 75 kHz sidescan sonar mosaic of individual clustered cold seeps. Note comet-tail-shaped reflections probably indicating gas bubble streams. High backscatter intensity is white. *Insert* Anomalies in the water column (gas flares) of unprocessed sidescan data that are displayed in reversed polarity

north, forming a major fossil cold seep that is connected in the subsurface (Fig. 4d). The fossil cold seep is characterised in sediment echosounder profiles by very strong amplitudes with highly reflective and diffuse subsurface echoes. Hyperbolic echoes suggest that the irregular surface of the cold seep is overlain by 5–15 m of well-stratified and weakly reflective deposits that correspond to low backscatter intensity of sidescan sonar records. The fossil cold seep shows a sharp northern boundary and a more progressive decrease in amplitudes towards the south, resulting in a total extension along the profile of 3,000 m. Seafloor observations of this fossil cold seep did not reveal signs of recent fluid venting activity but the presence of sediment-covered blocks of carbonate (Fig. 5d) suggests that fluid venting activity was present at these locations in the past. Indications for mass wasting deposits (Fig. 5e) have been observed and confirm the subbottom profiler data, suggesting that much of the cold seep facies has been buried under recent deposits (Fig. 4d).

The crest of the westernmost ridge located in 950 m water depth shows widespread indications for cold seeps in various stages of decline (Fig. 6c). Sediment echosounder profiles across the ridge (Fig. 4c) reveal a facies that is similar to cold seep facies in other parts of the study area. In particular, one profile shows a 20-m-high and 200× 400 m wide structure similar to those found in the area of Bio Bio Canyon. This area shows an irregular pattern of elevated backscatter intensity that reflects the rough surface of this fossil cold seep. Video observations revealed the presence of large carbonate blocks and carbonate pavements with epifauna, sea urchins and empty shells of vesicomyid clams (Fig. 5f, g), indicating that much of the ridge was formed by fluid venting but that methane emission has now ceased. However, in places tubeworms and bacterial mats suggesting active fluid venting are found in the close vicinity of the large carbonate blocks (Fig. 5g, h).

Other potential cold seeps

In comparison to Central America, the continental slope offshore central Chile does not show abundant mound structures. Seafloor mounds present at 36°26′S in 1,500 and 1,750 m depth may represent additional cold seeps. Here two rounded mounds several tens of metres in height and 1–2 km in diameter are present (Fig. 1). A similar feature, although much smaller, is located at 36°03'S/73°32'W. These features are morphologically similar to mound structures offshore Costa Rica, but their exact nature has not been determined.

The slump scars of large submarine landslides have been documented to host cold seeps (Mau et al. 2006). Bathymetric data indicate the presence of such submarine landslides on the lower continental slope offshore central Chile (Fig. 1). Whether these slump scars contain sites of fluid and gas emission cannot be determined from the present dataset.

Discussion

Cold seeps have been observed in various subduction zones, where they are generally concentrated in the forearc region. However, marked differences have been observed between

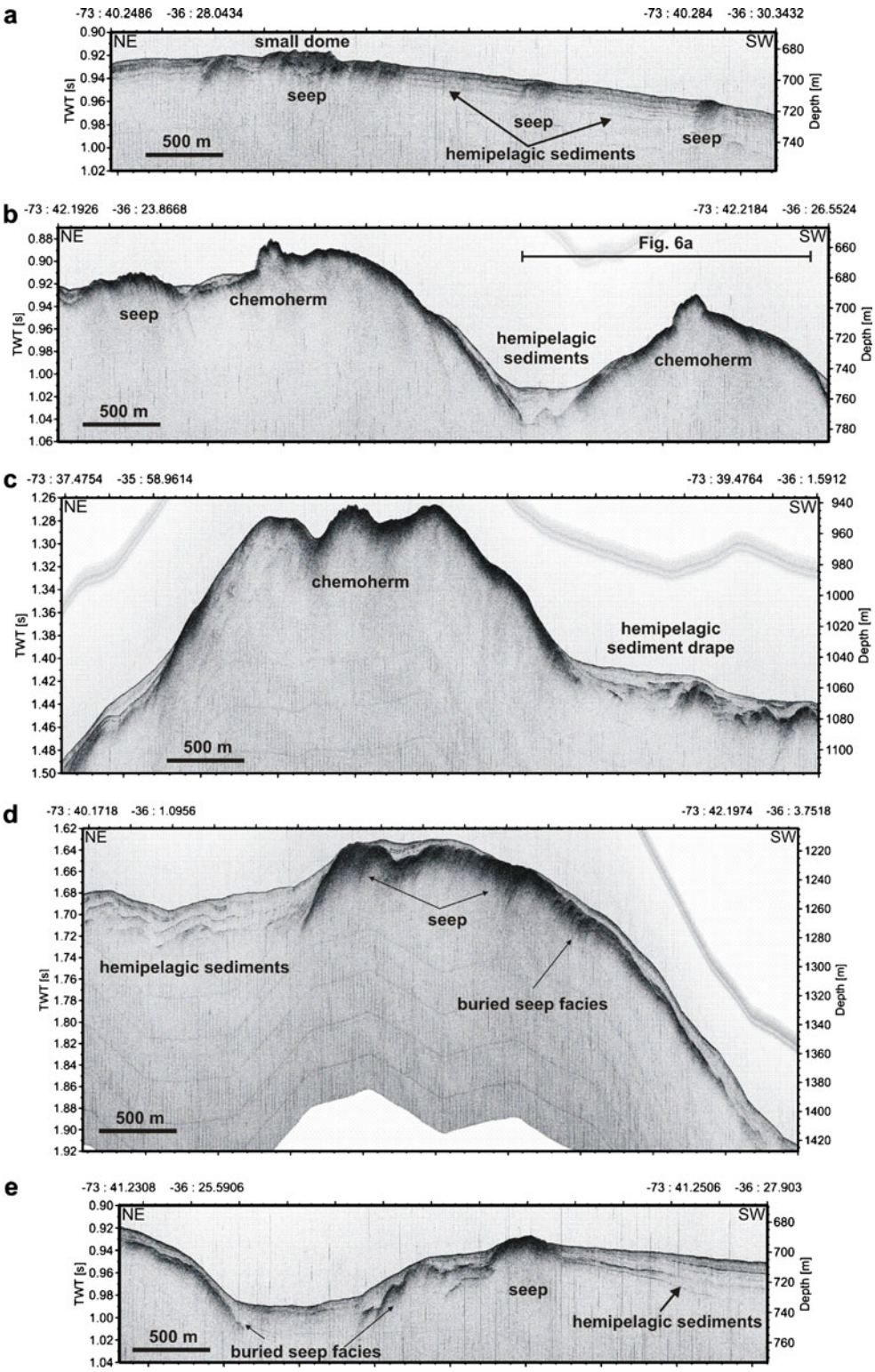

Fig. 4 2–8 kHz subbottom profiler records crossing cold seeps offshore central Chile. **a** Some of the clustered cold seeps with little or no relief (profile location in Fig. 3). **b** Widespread indications of gas and up to 20-m-high features extending above the surrounding seafloor (profile location in Fig. 6a). **c** Major ridge southwest of Itata Canyon, associated with strong bottom echoes with no penetration. The highly irregular seafloor at the northern end of the ridge probably represents a chemoherm similar to the profile in **b** (profile location in Fig. 6c). **d** Small ridge probably composed of authigenic carbonates (profile location in Fig. 6b). **e** Potential and largely sediment-covered cold seep in the vicinity of Itata Canyon (profile location in Fig. 6d)

erosional and accretionary margins. Cold seeps of the erosional Central American subduction zone are dominated by mound structures (Sahling et al. 2008) and normal faulting as pathways for fluids that are considered to have been generated at the plate interface (Hensen et al. 2004; Ranero et al. 2008). These seeps are found in a typical band of water depth and distance from the trench, continuous over hundreds of kilometres along slope (Sahling et al. 2008). In contrast, the central Chilean subduction zone, which is now accretionary (Bangs and Cande 1997), shows distinct clustering of fluid-escape features not unlike that described from other accretionary margins worldwide, such as

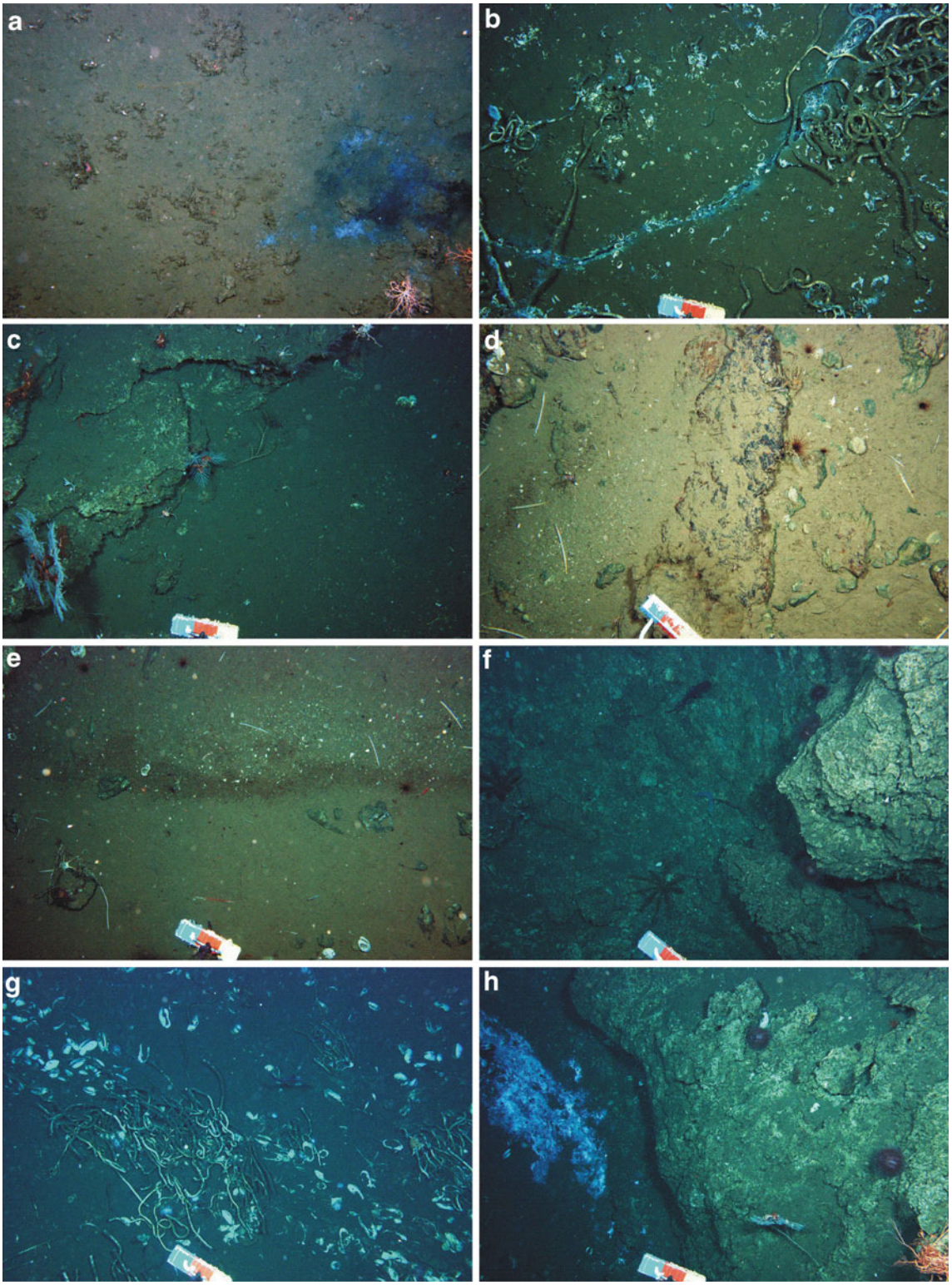

Fig. 5 Video observations of cold seeps along the central Chilean margin. The scale (ground weight) is 20 cm wide. **a** Patches of sulphidic sediment and bacterial mats. **b** Cracks in carbonate pavement with manifestations of fluid seepage (bacterial mats and tubeworms). **c** Base of the chemoherm in the south. **d** Sediment-covered block of carbonate. **e** Transported shell debris. **f** Large blocks of carbonate. **g** Shells of vesicomyid clams (*Archivesica* sp.) and large tubeworms of the genus *Lamellibrachia*. **h** Bacterial mats near a large carbonate block

Cascadia (Greinert et al. 2001; Johnson et al. 2003) and New Zealand (Greinert et al. 2010).

A full geochemical analysis of the fluids emanating at the central Chilean margin is still underway. However, first

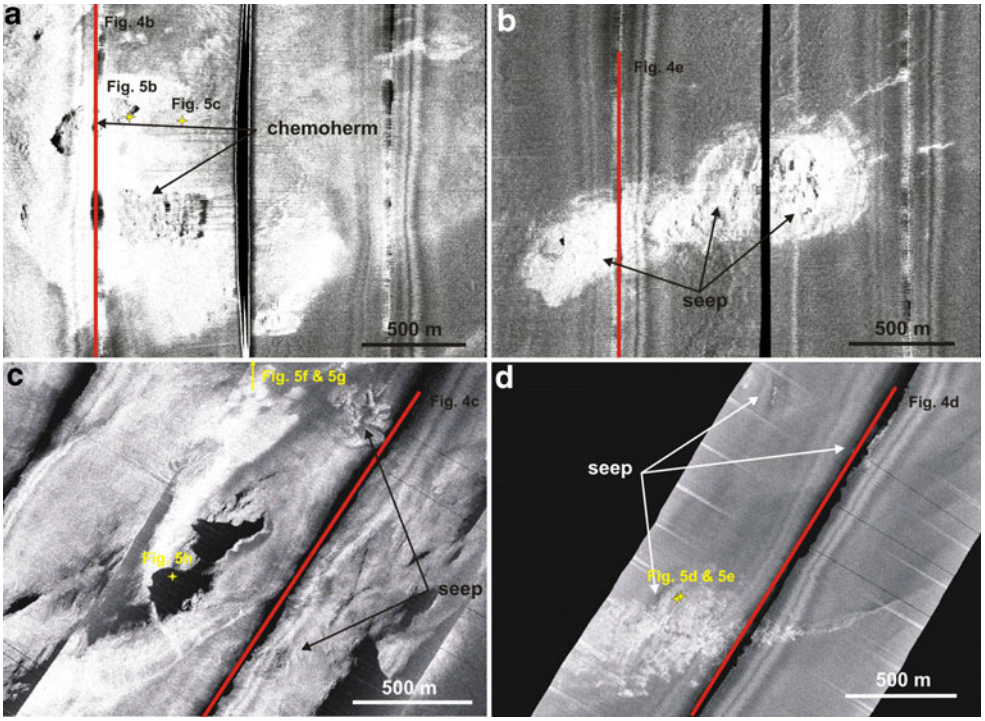

Fig. 6 75 kHz sidescan sonar images of cold seeps offshore Concepcion. High backscatter intensity is white. For locations, refer to Figs. 1 and 2. **a** Seeps with central chemoherm pinnacles. **b** Elongated ridge probably formed by fluid venting. **c** Small seeps and chemoherms on an accretionary ridge in the Itata area. Seafloor images in Fig. 5f and g are just a few hundred metres north of this map. **d** Potential cold seep in the vicinity of Itata Canyon

isotope analyses of the $\delta^{13}C$ of the carbonates that result from the microbially mediated anaerobic oxidation of methane and subsequent precipitation of the resulting, isotopically light CO_2 indicate values between −40 and −50‰ VPDB (V. Liebetrau, personal communication). These values suggest the methane to be of biogenic origin and probably generated within the slope sediments. Sellanes et al. (2008) report carbon isotopic values of −62.8±1.0‰ for gas hydrates and up to −52.65‰ for dissolved inorganic carbon within the porewater. This compares well with similar accretionary systems like the Cascadia subduction zone (Boetius and Suess 2004; Riedel et al. 2006) and the Hikurangi margin (Faure et al. 2010) where fluids are mainly biogenic in origin. In addition, the observation of gas flares offshore central Chile indicates that these systems are probably more active with higher fluid expulsion rates than those offshore Central America, where no such flares have been observed. Higher fluid expulsion rates at accretionary margins compared to erosional margins have also been documented by direct measurements at Hydrate Ridge and offshore New Zealand (Torres et al. 2002; Sommer et al. 2010). Most likely, the presence of possible chemoherm structures offshore Chile (Figs. 4b, c, 6a, c) supports the idea of high and prolonged fluid flux, as the formation of chemoherms requires a high methane flux that moves the sulphate–methane interface into the water column (Luff and Wallmann 2003) and consequently enables the growth of authigenic carbonates into the water column, as suggested for the chemoherm structures on Hydrate Ridge (Teichert et al. 2005). The central Chilean subduction zone, therefore, shows cold seep structures and characteristics typical of accretionary margins. Chemoherm build-ups are common features on Hydrate Ridge (Greinert et al. 2001; Teichert et al. 2005), and active gas emission in the form of gas bubbles has been described from both Hydrate Ridge (Heeschen et al. 2003) and New Zealand (Klaucke et al. 2010). However, in these two areas cold seeps are located at the top of accretionary ridges (Johnson et al. 2003; Barnes et al. 2010) whereas, offshore Chile, cold seeps appear to be concentrated at the margin of intraslope basins.

The cold seeps offshore Chile show indications for active fluid venting in the form of acoustic anomalies in the water column (Fig. 3a) and bacterial mats covering the seafloor (Fig. 5a, h). However, compared to the extent of high backscatter anomalies on the seafloor that reflect authigenic carbonate precipitates, these manifestations of currently active cold seeps are scarce. Most of the cold seeps offshore Chile described here are consequently fossil seeps and point to either much higher fluid fluxes in the past or fluid flux over prolonged periods. Particularly the massive carbonate accumulations of chemoherm build-ups (Figs. 3 and 4) that are morphologically similar to chemoherm structures described offshore Oregon (Greinert et al. 2001; Teichert et al. 2005) require both strong and prolonged fluid flux, unless they represent the exposed plumbing system of individual cold seeps. Indications for strong erosion such as reported for large mound structures offshore Central America (Buerk et al. 2010) are absent offshore Chile. Whether higher fluid flux during sea-level lowstands (Teichert et al. 2003; Kiel 2009) or prolonged fluid flux with potentially migrating or shifting centres of fluid venting activity

explains the extent of fossil cold seeps offshore Chile can only be elucidated by dating various authigenic carbonate precipitates (Liebetrau et al. 2010).

Conclusions

Geoacoustic data have shown the presence of large areas covered by cold seeps in 600 to 1,000 m water depth along the upper continental slope offshore central Chile. At least some of these sites are presently active but seep activity must have been more intense in the past. This significantly expands known occurrences of both fossil and active cold seeps in this area. Observed fossil and active cold seep morphologies and characteristics range from isolated, rounded high-backscatter anomalies, to clusters of such anomalies, chemoherm structures, fault traces and potentially entire ridges that were partially formed or have been overprinted by fluid venting and authigenic carbonate formation. Much of the continental margin offshore central Chile also shows the presence of a bottom simulating reflector that is disrupted and bent upwards at the sites of the cold seeps. Judging by their extent and the concentration of mainly fossil cold seeps, these sites are among the largest cold seep areas at active continental margins known to date. Age and lifespan of the fossil cold seeps are not known, but fluid flow activity might have been much higher during sea-level lowstands than today.

Acknowledgements Cruise JC23 of RRS *James Cook* has been made possible through the OFEG barter programme. Cruise SO210 of RV *Sonne* was conducted by ship time exchange with RV *Meteor*. We would like to thank the captains, officers and crews of both vessels for their help and great professionalism at sea. Reviews by T. Lorenson and G. Westbrook helped improving the manuscript. This is contribution 221 of the Sonderforschungsbereich (SFB) 574 "Volatiles and fluids in subduction zones" at Kiel University. SFB 574 is financed by the German Research Foundation (DFG).

References

Bangs NL, Cande SC (1997) Episodic development of a convergent margin inferred from structures and processes along the southern Chile margin. Tectonics 16:489–503

Barnes PM, Lamarche G, Bialas J, Henrys S, Pecher I, Netzeband GL, Greinert J, Mountjoy JJ, Pedley K, Crutchley G (2010) Tectonic and geological framework for gas hydrates and cold seeps on the Hikurangi subduction margin, New Zealand. Mar Geol 272:26–48

Behrmann JH (1992) Conditions for hydrofracture and the fluid permeability of accretionary prisms. Earth Plant Sci Lett 107:550–558

Boetius A, Suess E (2004) Hydrate Ridge: a natural laboratory for the study of microbial life fuelled by methane from near-surface gas hydrates. Chem Geol 205:291–310

Buerk D, Klaucke I, Sahling H, Weinrebe W (2010) Morpho-acoustic variability of cold seeps on the continental slope offshore Nicaragua: result of fluid flow interaction with sedimentary processes. Mar Geol 275:53–65

Carson B, Screaton EJ (1998) Fluid flow in accretionary prisms: evidence for focused, time-variable discharge. Rev Geophys 36:329–352

Crutchley GJ, Geiger S, Pecher IA, Gorman AR, Zhu H, Henrys SA (2010) The potential influence of shallow gas and gas hydrates on sea floor erosion of Rock Garden, an uplifted ridge offshore of New Zealand. Geo-Mar Lett 30:283–303. doi:10.1007/s00367-010-0186-y

DeMets C, Gordon RG, Argus DF, Stein S (1994) Effect of recent revisions to the geomagnetic reversal time scale on estimates of current plate motions. Geophys Res Lett 21:2191–2194

Dugan B, Flemings PB (2000) Overpressure and fluid flow in the New Jersey continental slope: implications for slope failure and cold seeps. Science 289:288–291

Faure K, Greinert J, Schneider von Deimling J, McGinnis DF, Kipfer R, Linke P (2010) Methane seepage along the Hikurangi Margin of New Zealand: geochemical and physical data from the water column, sea surface and atmosphere. Mar Geol 272:170–188

Geersen J, Völker D, Krastel-Gudegast S, Diaz J, Weinrebe RW, Behrmann JH (2011) Active tectonics of the South Chilean marine forearc (35°S – 40°S). Tectonics 30:TC3006. doi:10.1029/2010TC002777

Greinert J, Bohrmann G, Suess E (2001) Gas hydrate-associated carbonates and methane-venting at Hydrate Ridge: classification, distribution and origin of authigenic lithologies. In: Paull CK, Dillon PW (eds) Natural gas hydrates: occurrence, distribution, and detection. AGU Geophys Monogr 124:99–113

Greinert J, Lewis K, Bialas J, Pecher I, Rowden A, Linke P, De Batist M, Bowden D, Suess E (2010) Methane seepage along the Hikurangi Margin, New Zealand: review of studies in 2006 and 2007 and new evidence from visual, bathymetric and hydroacoustic investigations. Mar Geol 272:6–25

Heeschen KU, Tréhu AM, Collier RW, Suess E, Rehder G (2003) Distribution and height of methane bubble plumes on the Cascadia Margin characterized by acoustic imaging. Geophys Res Lett 30:1643. doi:10.1029/2003GL016974

Henry P, Le Pichon X, Lallemant S, Foucher JP, Westbrook GK, Hobart M (1990) Mud volcano field seaward of the Barbados Accretionary Complex: a deep towed sidescan sonar survey. J Geophys Res 95B:8917–8929

Henry P, Lallemant S, Nakamura K, Tsunogai U, Mazzotti S, Kobayashi K (2002) Surface expression of fluid venting at the toe of the Nankai wedge and implications for flow paths. Mar Geol 187:119–143

Hensen C, Wallmann K, Schmidt M, Ranero CR, Suess E (2004) Fluid expulsion related to mud extrusion off Costa Rica - a window to the subducting slab. Geology 32:201–204

Hubbert MK, Rubey WW (1959) Role of fluid pressure in the mechanics of overthrust faulting. I: mechanics of fluid filled porous solids and its applications to overthrust faulting. Geol Soc Am Bull 70:115–166

Johnson JE, Goldfinger C, Suess E (2003) Geophysical constraints on the surface distribution of authigenic carbonates across the Hydrate Ridge region, Cascadia margin. Mar Geol 202:79–120

Kiel S (2009) Global hydrocarbon seep-carbonate precipitation correlates with deep-water temperatures and eustatic sea-level fluctuations since the Late Jurassic. Terra Nova 21:279–284

Klaucke I, Sahling H, Bürk D, Weinrebe RW, Bohrmann G (2005) Mapping deep-water gas emissions with sidescan sonar. Eos 86:341–346

Klaucke I, Weinrebe RW, Petersen CJ, Bowen DA (2010) Temporal variability of gas seeps offshore New Zealand: multi-frequency

geoacoustic imaging of the Wairarapa area, Hikurangi margin. Mar Geol 272:49–58

Kobayashi K (2002) Tectonic significance of the cold seepage zones in the Eastern Nankai Accretionary Wedge: an outcome of the 15 years' KAIKO projects. Mar Geol 187:3–30

Kukowski N, Oncken O (2006) Subduction erosion—The "normal" mode of fore-arc material transfer along the Chilean Margin? In: Oncken O, Chong G, Franz G, Giese F, Götze H-J, Ramos VA, Strecker ME, Wigger P (eds) The Andes: active subduction orogeny. Springer, Berlin, pp 217–236

Le Bas TP, Mason DC, Millard NW (1995) TOBI image processing - the state of the art. IEEE J Ocean Eng 20:85–93

Liebetrau V, Eisenhauer A, Linke P (2010) Cold seep carbonates and associated cold-water corals at the Hikurangi Margin, New Zealand: new insights into fluid pathways, growth structures and geochronology. Mar Geol 272:307–318

Luff R, Wallmann K (2003) Fluid flow, methane fluxes, carbonate precipitation and biogeochemical turnover in gas hydrate-bearing sediments at Hydrate Ridge, Cascadia margin: numerical modelling and mass balances. Geochim Cosmochim Acta 67:3403–3421

Mau S, Sahling H, Rehder G, Suess E, Linke P, Soeding E (2006) Estimates of methane output from mud extrusions at the erosive convergent margin off Costa Rica. Mar Geol 225:129–144

Melnick D, Echtler HP (2006) Inversion of forearc basins in south-central Chile caused by rapid glacial age trench fill. Geology 34:709–712

Miller SA (2002) Properties of large ruptures and the dynamical influence of fluids on earthquakes and faulting. J Geophys Res 107(B9):2182. doi:10.1029/2000JB00003

Moore JC, Vrolijk P (1992) Fluids in accretionary prisms. Rev Geophys 30:113–135

Paull CK, Hecker B, Commeau R, Freeman-Lynde RP, Neumann C, Corso WP, Golubic S, Hook JE, Sikes E, Curray J (1984) Biological communities at the Florida escarpment resemble hydrothermal vent taxa. Science 226:965–967

Ranero CR, Grevemeyer I, Sahling H, Barckhausen U, Hensen C, Wallmann K, Weinrebe RW, Vannucchi P, von Huene R, McIntosh K (2008) The hydrogeological system of erosional convergent margins and its influence on tectonics and interplate seismogenesis. Geochem Geophys Geosyst 9:Q03S04. doi:10.1029/2007GC001679

Riedel M, Novosel I, Spence GD, Hyndman RD, Chapman NR, Solem RC, Lewis T (2006) Geophysical and geochemical signatures associated with gas hydrate related venting at the north Cascadia margin. Geol Soc Am Bull 118:23–38

Sahling H, Masson DG, Ranero CR, Hühnerbach V, Weinrebe RW, Klaucke I, Bürk D, Brückmann W, Suess E (2008) Fluid seepage at the continental margin off Costa Rica and Nicaragua. Geochem Geophys Geosyst 9:Q05S05. doi:10.1029/2008GC001978

Sellanes J, Quiroga E, Neira C (2008) Megafaunal community structure and trophic relationships of the recently discovered Concepcion Methane Seep Area (Chile, 36°S). ICES J Mar Sci 65:1102–1111

Sellanes J, Neira C, Quiroga E, Teixido N (2010) Diversity patterns along and across the Chilean margin: a continental slope encompassing oxygen gradients and methane seep benthic habitats. Mar Ecol 31:111–124

Sommer S, Linke P, Pfannkuche O, Niemann H, Treude T (2010) Benthic respiration in a seep habitat dominated by dense beds of ampharetid polychaetes at the Hikurangi Margin (New Zealand). Mar Geol 272:223–232

Sultan N, Cochonat P, Canals M, Cattaneo A, Dennielou B, Haflidason H, Laberg JS, Long D, Mienert J, Trincardi F (2004) Triggering mechanisms of slope instability processes and sediment failures on continental margins: a geotechnical approach. Mar Geol 213:291–321

Teichert BMA, Eisenhauer A, Bohrmann G, Haase-Schramm A, Bock B, Linke P (2003) U/Th systematics and ages of authigenic carbonates from Hydrate Ridge, Cascadia Margin: recorders of fluid flow variations. Geochim Cosmochim Acta 67:3845–3857

Teichert BMA, Bohrmann G, Suess E (2005) Chemoherms on Hydrate Ridge - unique microbially-mediated carbonate build-ups growing into the water column. Palaeogeogr Palaeoclimatol Palaeoecol 227:67–85

Thornburg TM, Kulm LD, Hussong DM (1990) Submarine-fan development in the southern Chile Trench: a dynamic interplay of tectonics and sedimentation. Geol Soc Am Bull 102:1658–1680

Torres ME, McManus J, Hammond DE, de Angelis MA, Heeschen KU, Colbert SL, Tryon MD, Brown KM, Suess E (2002) Fluid and chemical fluxes in and out of sediments hosting methane hydrate deposits on Hydrate Ridge, OR, I: hydrological provinces. Earth Planet Sci Lett 201:525–540